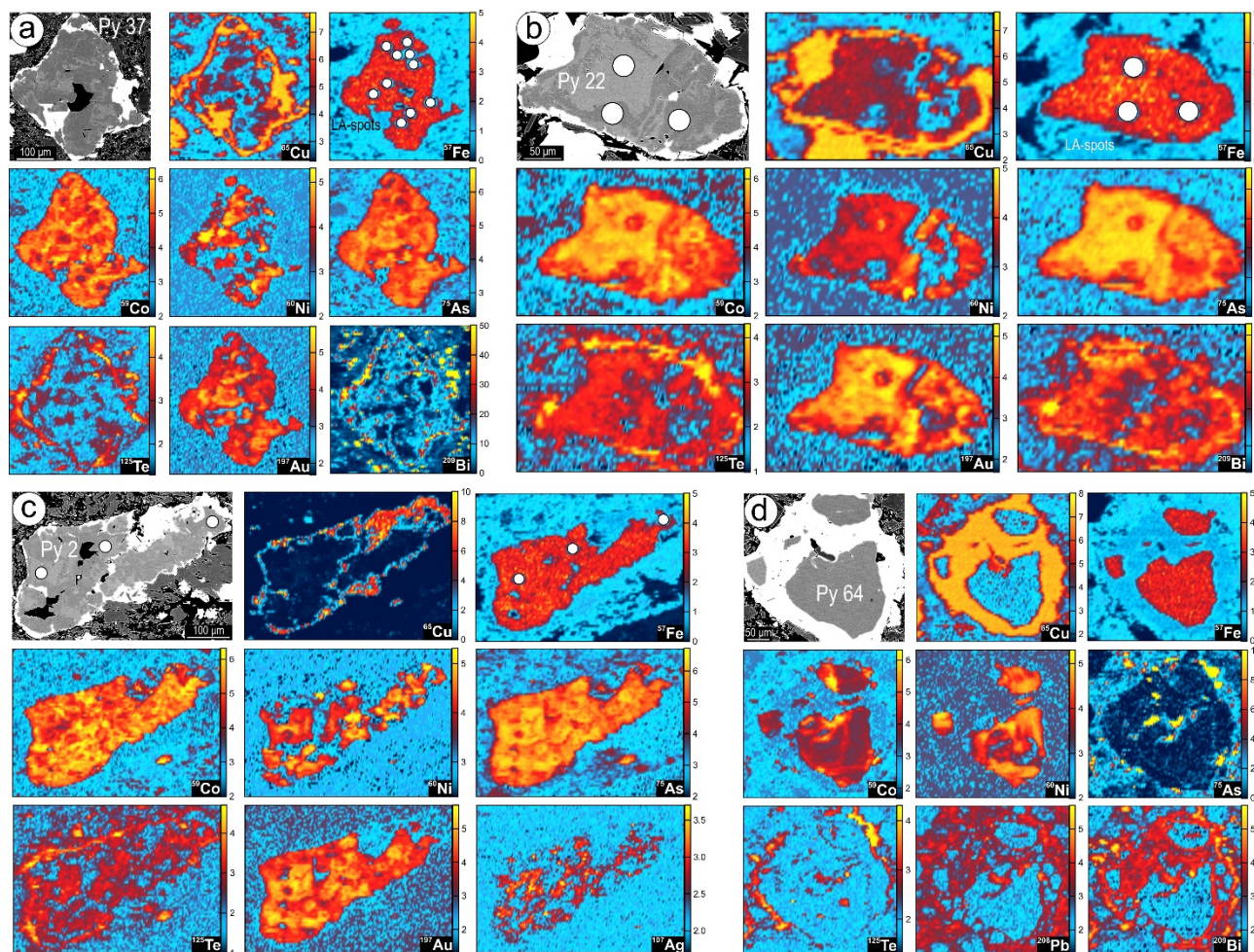


ONLINE MATERIALS



**Figure. A1.** BSE images and LA-ICPMS maps (scales in counts per second, cps,  $10^n$ ) for pyrites showing major (Cu, Fe) and trace element distributions at the micron-scale. Py# numbers correspond to those shown in Figure 1a. White circles are spot analyses from Dataset 2 in Online Material<sup>1</sup> Table A1. (a-c) As-Au-bearing pyrites showing relative correlation between Au and As. Note the presence of other elements overlapping with Au (Bi in b, Te, and Ag in c). (d) Au-As-poor pyrite with advanced replacement by chalcopyrite. Note preservation of Co and Ni patterns whereas elements such as Te, Pb and Bi are concentrated within or at the boundaries of chalcopyrite (bright on the BSE images).

**Methodology**

LA-ICP-MS element maps were obtained for subsets of analyzed isotopes (Online Material<sup>1</sup> Table A1) from grids of parallel lines ablated across the selected areas using a fluence of  $\sim 3 \text{ J/cm}^2$  and laser repetition rates of 10 Hz. Spot sizes of 7 and 11  $\mu\text{m}$  was used with speeds of 7 and 11  $\mu\text{m/s}$ , respectively. Prior to the main ablation and signal acquisition phase, individual lines were pre-ablated to clean the surfaces and minimize the contributions from ablation blankets of the previous lines. A 20s background acquisition for each line was conducted prior to the main ablation. Spot analyses were conducted on reference materials before and after each mapping run. Data reduction was conducted in Iolite. Individual line-profiles of the measured isotopes were merged into 2D-images by subtracting the average backgrounds from the time-resolved intensities and producing qualitative isotope intensity maps with scales in counts-per-second (cps). The obtained intensities were scaled individually to highlight intragrain variability.

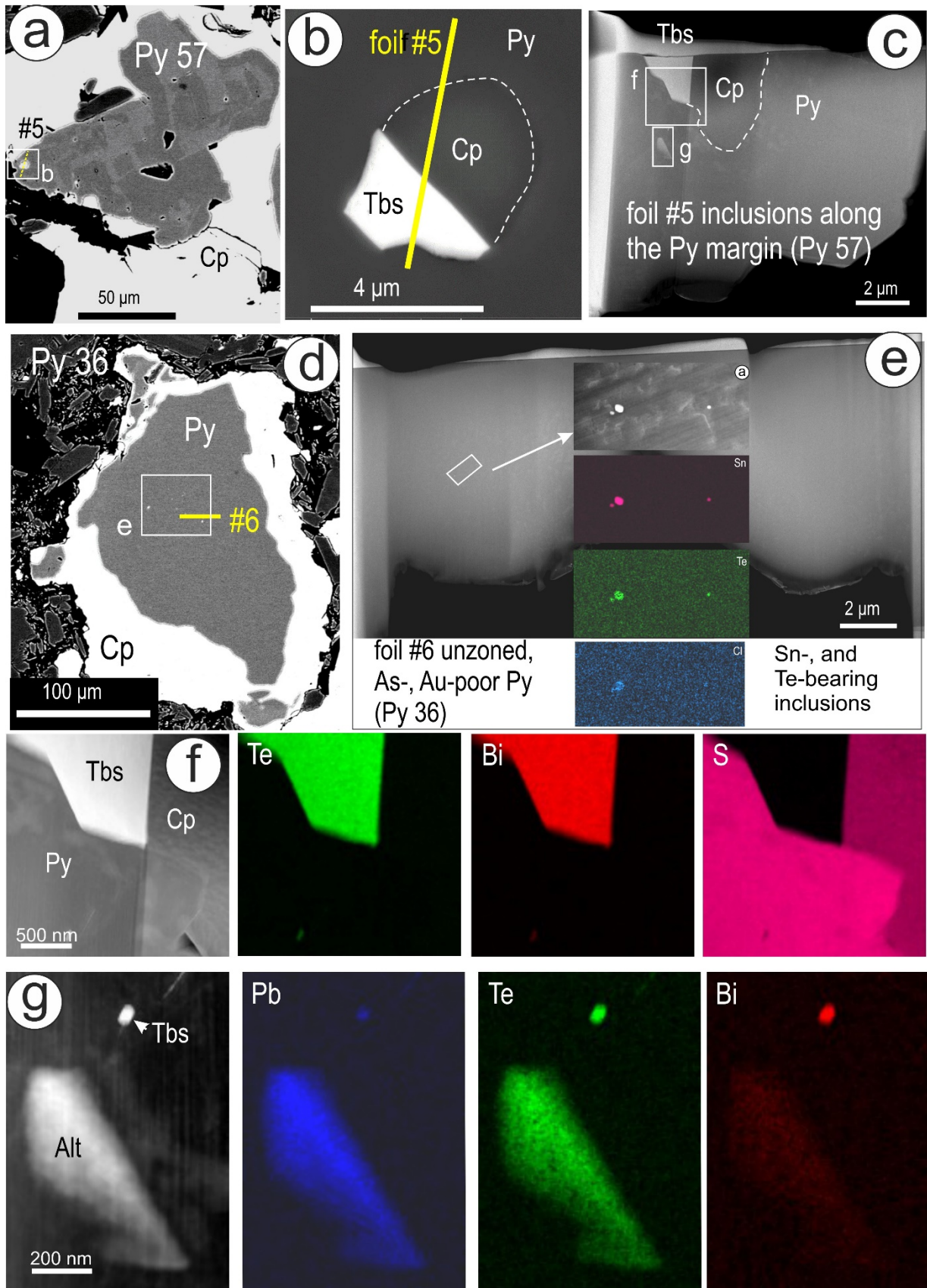


**Figure A2.** BSE (a, b, d) of two other grains of pyrite that were sampled for nanoscale analysis (FIB cuts as yellow lines). Micron-sized inclusion of tellurobismuthite (Tbs) associated with chalcopyrite (Cp) towards the margin of Py57. (c, e) HAADF STEM images of foils obtained from the FIB cuts. Pyrite 36 in (d, e) is As-Au-poor but contains Sn. STEM EDS maps as overlays in (e) showing the presence of cassiterite inclusions; Te and Cl are also present. (f, g) Images and STEM EDS maps of the tellurobismuthite inclusion in (b) and altaite (Alt; PbTe) below the large Tbs [maps marked in (c)]. Note the presence of Tbs NPs adjacent to altaite.

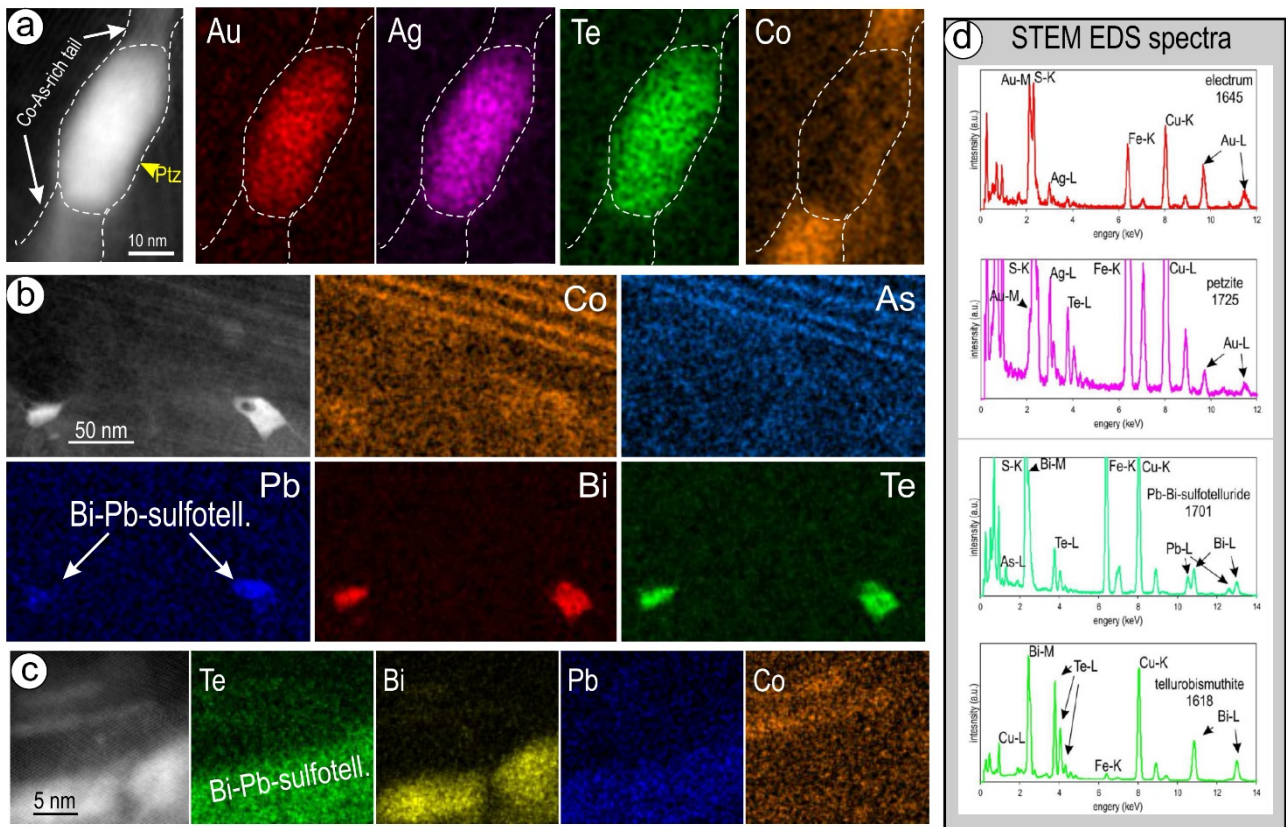


**Figure A3.** (a-c) HAADF STEM images and STEM EDS maps of Au-Ag-tellurides (a), and Bi-Pb-sulfotellurides (b, c) from Py67a. Note the presence of Co and lesser concentrations of As along or adjacent to NPs. (d) STEM RDS spectra of representative inclusions as marked.

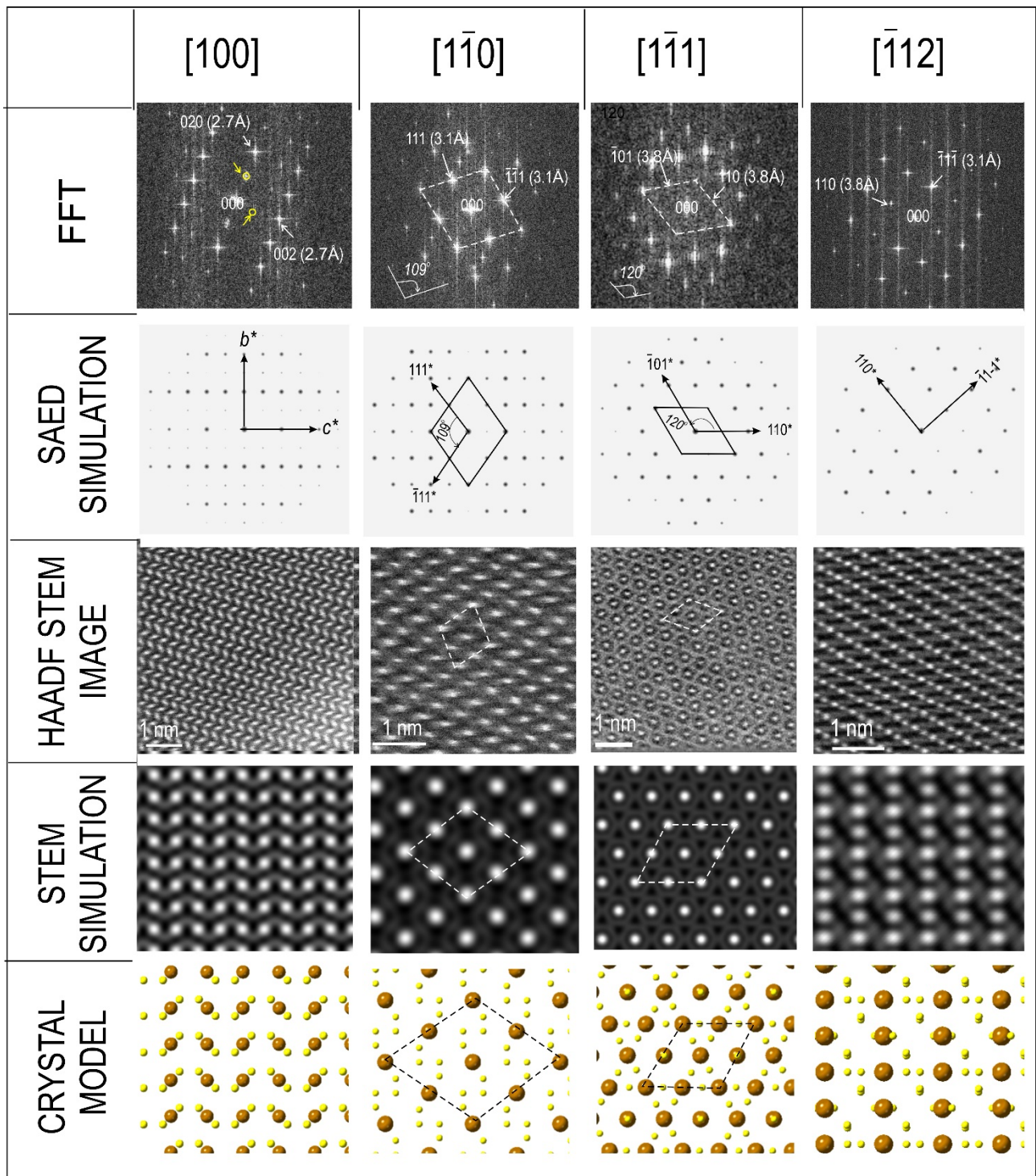


**Figure A4.** FFT, electron diffraction (SAED) patterns, HAADF STEM images, simulations and atom-fill crystal models as labelled, showing pyrite on four main zone axes. Indexing using the *P*-1 space group from Bayliss (1977). Atoms in the crystal models: brown=Fe, yellow=S.